Polymer 52 (2011) 987–995

Contents lists available at ScienceDirect

Polymer

journal homepage: www.elsevier.com/locate/polymer

Poly(acrylic acid)-grafted magnetic nanoparticle for conjugation with folic acid

Metha Rutnakornpituk*, Nipaporn Puangsin, Pawinee Theamdee, Boonjira Rutnakornpituk, Uthai Wichai

Department of Chemistry and Center of Excellence for Innovation in Chemistry, Faculty of Science, Naresuan University, Phitsanulok 65000, Thailand

ARTICLE INFO

Article history:
Received 7 October 2010
Received in revised form
22 December 2010
Accepted 24 December 2010
Available online 9 January 2011

Keywords:
Nanoparticle
poly(acrylic acid)
ATRP

ABSTRACT

Poly(acrylic acid) (poly(AA))-grafted magnetite nanoparticles (MNPs) prepared *via* surface-initiated atom transfer radical polymerization (ATRP) of *t*-butyl acrylate, followed by acid-catalyzed deprotection of *t*–butyl groups, is herein presented. In addition to serve as both steric and electrostatic stabilizers, poly(AA) grafted on MNP surface also served as a platform for conjugating folic acid, a cancer cell targeting agent. Fourier transform infrared spectroscopy (FTIR) was used to monitor the reaction progress in each step of the syntheses. The particle size was 8 nm in diameter without significant aggregation during the preparation process. Photocorrelation spectroscopy (PCS) indicated that, as increasing pH of the dispersions, their hydrodynamic diameter was decreased and negatively charge surface was obtained. According to thermogravimetric analysis (TGA), up to 14 wt% of folic acid (about 400 molecules of folic acid per particle) was bound to the surface-modified MNPs. This novel nanocomplex is hypothetically viable to efficiently graft other affinity molecules on their surfaces and thus might be suitable for use as an efficient drug delivery vehicle particularly for cancer treatment.

1. Introduction

Synthesis of magnetite nanoparticles (MNPs) coated with a thin film of organic polymer has recently attracted much attention due to their potential biomedical applications such as magnetic resonance imaging [1–6], magnetic separation, controlled drug release [7] and hyperthermia treatment of tumor cells [8]. A thin shell of polymeric coating on the particle surface is necessary to prevent nanometer-sized particle aggregation due to their inherent anisotropic dipolar interaction, resulting in losing the specific properties associated with their nanometer dimensions [9,10]. In addition, the polymers on their surface can provide a platform for incorporating biological functional molecules, such as amino acid [11], protein [12,13] and DNA [14–16], for particle labeling with fluorescent molecules [10,17] and for attaching folic acid [18,19], a receptor for tumor cells.

Recently, atom transfer radical polymerization (ATRP) has been reported as a potential "grafting-from" method for surface modification [20,21,27]. ATRP is a living/controlled radical polymerization method, which does not require stringent experimental conditions [22,23]. ATRP enables for the polymerization and block copolymerization of a wide range of functional monomers such as styrene [24–26], methacrylate [27], acrylate [28,29] and methacrylamide [30], yielding polymers with narrowly dispersed molecular weights. Surface modification of nanoparticles *via* ATRP has attracted a great attention in recent years. As compared to a conventional radical polymerization, surface-initiated ATRP from nanoparticles produced polymers with narrow polydispersity index (PDI) and proceeded in a controlled fashion [31]. In addition, the advantage of ATRP technique as compared to other controlled radical polymerization (CRP) techniques is that the polymerization can be initiated at low reaction temperature, while other CRP techniques such as reversible addition-fragmentation chain transfer (RAFT) and nitroxide-mediated polymerizations require relatively high reaction temperature to generate radicals from azo or peroxide initiators. Moreover, functionalization of the particle surface with alkyl halide, the ATRP initiating species, can be easily carried out either by physical absorption of acid-containing halides [36] or covalent bonding of ATRP initiating halides *via* silanization [32]. The "grafting from" strategy *via* ATRP has thus been mostly adopted for MNP surface modification with a variety of polymeric surfactants such as polystyrene [27], poly(methyl methacrylate) [33], poly(ethylene glycol) methacylate [34,35] and poly(acrylamide) [36].

The aim of the current work is to adopt a "grafting from" method to modify MNP surfaces with poly(*t*-butyl acrylate) (poly(*t*-BA)) *via* ATRP, followed by acid-catalyzed deprotection of *t*-butyl groups to obtain poly(AA)-grafted MNP. It is thought that ATRP can offer well-defined water dispersible poly(AA) stabilizers with low molecular weight distribution on the particle surface. The carboxylic acid groups overexpressed on its surface are readily reactive toward molecules containing functional groups such as amine and alcohol. It has thus gained our attention because, not only serving as steric and electrostatic surfactants [37], poly(AA) can also be used as a key intermediate

* Corresponding author. Tel.: +66 5596 3464; fax: +66 5596 1025.
E-mail address: methar@nu.ac.th (M. Rutnakornpituk).

0032-3861/$ – see front matter © 2011 Elsevier Ltd. All rights reserved.
doi:10.1016/j.polymer.2010.12.059

for grafting a large range of functional molecules [38,39]. Folic acid (FA) is of particular interest in this work because it can specifically conjugate with folate receptors overexpressed on cancer cell membranes [40]. Precedents have reported the immobilization of FA on the outermost surface of MNPs coated with other polymeric surfactants [41–44]. Therefore, it is expected that the multifunctional FA-grafted MNPs prepared in this work should bind to cancer cell membranes specifically and consequently improve uptake efficiency of the MNP to the cells. The detail studies on the efficiency on treating cancer cells of this complex are warranted for a future investigation.

In the present work, poly(AA)-coated MNPs were thus prepared *via* surface-initiated ATRP of *t*-BA, followed by acid-catalyzed hydrolysis of *t*-butyl groups. FTIR was used to monitor the reaction progress in each step. Thermogravimetric analysis (TGA) was used to investigate percent of each composition in the polymer-MNP complex. Transmission electron microscopy (TEM) technique was also used to monitor the particle size and the presence of the polymer in the complex. Vibrating sample magnetometry (VSM) was performed to reveal their magnetic properties. In combination with UV–visible spectrophotometry and FTIR, TGA technique was conducted to evidence the existence of FA in the complexes.

2. Experimental section

2.1. Materials

Unless otherwise stated, all reagents were used without further purification: iron (III) acetylacetonate ($Fe(acac)_3$), 99% (Acros), benzyl alcohol (Unilab), 3-aminopropyl triethoxysilane (APS), 99% (Acros), triethylamine (TEA) (Carto Erba), 2-bromoisobutyryl bromide (BIBB), 98% (Acros), copper (I) bromide (CuBr), 98% (Acros), *N,N,N′,N″,N″*-pentamethyldiethylenetriamine (PMDETA), ethyl-α-bromoisobutyrate (Aldrich), 99% (Acros), folic acid, 97% (Fluka), N-hydroxyl succinamide (NHS), 98% (Acros), dicyclohexyl carbodiimide (DCC), 99% (Acros), di-*t*-butyl dicarbonate (Boc_2O), 99% (Aldrich), ethylene diamine (EDA), 99.5% (Fluka), trifluoroacetic acid (TFA), 99.5% (Fluka). *t*-Butyl acrylate (*t*-BA), 99% (Fluka), was distilled under vacuum prior to use.

2.2. Synthesis

2.2.1. Synthesis of oleic acid-coated magnetite nanoparticles (MNPs)

MNPs were prepared *via* thermal decomposition following the method previously described [45]. In a typical procedure, $Fe(acac)_3$ (1.0 g, 2.81 mmol) and benzyl alcohol (20 ml) were mixed by magnetic stirring in a three-neck flask with nitrogen flow. The mixture was heated to 200 °C for 48 h. The precipitant was then removed from the dispersion using an external magnet and washed with ethanol and CH_2Cl_2 repeatedly to remove benzyl alcohol. The particles were then dried at room temperature under reduced pressure. To prepare oleic acid-coated MNPs, the dried MNPs (0.6 g) were introduced into an oleic acid solution in dried toluene (4 ml oleic acid in 30 ml THF) and ultrasonicated for 3 h.

2.2.2. Synthesis of 2-bromo-2-methyl-N-(3-(triethoxysilyl) propanamide (BTPAm))

To a stirred solution of 3-aminopropyl triethoxysilane (APS) (0.18 ml, 0.8 mmol) and triethylamine (TEA) (0.12 ml, 0.8 mmol) in dried toluene (10 ml), 2-bromoisobutyryl bromide (BIBB) (0.1 ml, 0.8 mmol) in dried toluene (10 ml) was added dropwise at 0 °C for 2 h under nitrogen. The reaction mixture was warmed to room temperature and stirred for 24 h. The mixture was passed through a filter paper to remove salts and the filtrate was evaporated to remove the unreacted TEA under reduced pressure. The resulting product, BTPAm, was yellowish thick liquid (78% yield). ^{1}H NMR (400 MHz, $CDCl_3$) δ_H: 0.60 [m, 2H, Si–C<u>H</u>$_2$, 1.20 [t, 9H, O–CH$_2$–C<u>H</u>$_3$], 1.65 [m, 2H, Si–CH$_2$–C<u>H</u>$_2$], 1.95, [s, 6H, C<u>H</u>$_3$–C–Br], 3.25 [m, 2H, C<u>H</u>$_2$–NH], 3.80 [m, 6H, CH$_3$–C<u>H</u>$_2$–O]. FT-IR (KBr disc) υ_{max}: 3345 cm^{-1} (NH stretching), 2975–2889 cm^{-1} (C–H stretching), 1738 cm^{-1} (C=O of acid bromide stretching), 1658 cm^{-1} (C=O of amide stretching), 1532 cm^{-1} (NH bending), 1442 cm^{-1} (C–N stretching), 1286 cm^{-1} (C–Br stretching), 1112–1026 (Si–O stretching).

2.2.3. Immobilization of 2-bromo-2-methyl-N-(3-(triethoxysilyl) propanamide (BTPAm)) onto MNP surface (BTPAm-coated MNPs) (Fig. 1)

To immobilize BTPAm on the oleic acid-coated MNP surface, the MNP-toluene dispersion (0.1 g of oleic acid-coated MNPs in 5 ml toluene) (30 ml), BTPAm (0.90 ml) and 2 M TEA in toluene (6 ml) were added into a round bottom flask. The mixture was stirred for 24 h at room temperature under nitrogen. The particles were subsequently precipitated in methanol, following by magnet separation to obtain the BTPAm-modified MNPs. Then, the MNPs were re-dispersed in toluene and re-precipitated in methanol. This procedure was repeated several times to completely remove unreacted BTPAm. The particles were finally dried *in vacuo*.

2.2.4. Synthesis of poly(t-butyl acrylate)-coated MNPs (poly(t-BA)-coated MNPs) via ATRP reaction

To a schlenk tube containing dioxane (1 ml), CuBr (0.3 g, 0.0021 mol), and PMDETA (0.42 ml, 0.0021 mol) were added under nitrogen blanket. The mixture was stirred until homogenous blue color was observed. Then, *t*-butyl acrylate (*t*-BA) (3 ml, 0.021 mol) monomer and BTPAm-immobilized MNPs (0.3 g) were added *via* a syringe. The mixture was degassed and nitrogen-purged by three freeze-thaw cycles. The solution was then heated to 90 °C for 24 h to commence ATRP reaction. At a given time, the reactions were ceased and poly(*t*-BA)-grafted MNPs were magnetically separated and washed thoroughly with methanol and dried *in vacuo*.

2.2.5. Synthesis of poly(acrylic acid)-coated MNPs (poly(AA)-coated MNPs) via hydrolysis of poly(t-butyl acrylate)-coated MNPs

Poly(*t*-BA)-coated MNPs were hydrolyzed to obtain acrylic acid functional groups on MNP surfaces. Briefly, poly(*t*-BA)-coated MNPs (0.05 g) were hydrolyzed in a 20-ml TFA solution (0.1 M of TFA in THF) at room temperature for 24 h. The solution was concentrated under reduced pressure, diluted with CH_2Cl_2, and repeatedly precipitated in cold hexane. The precipitate was separated by a permanent magnet and dried *in vacuo*. The possible reactions between TFA and polymers coated on MNP surface are illustrated in supplementary data.

2.2.6. Synthesis of N-(2-aminoethyl) folic acid (EDA-FA) (Fig. 2)

2.2.6.1. Protection of an amino group of ethylene diamine (EDA) with t-butyl carbamate (Boc). A solution of di-*t*-butyl dicarbonate (Boc_2O) (0.23 ml, 1 mmol) in anhydrous CH_2Cl_2 (10 ml) was added dropwise to a cold solution of ethylene diamine (EDA) (0.67 ml, 10 mmol) in anhydrous CH_2Cl_2 (10 ml) at 0 °C under nitrogen atmosphere. The mixture was magnetically stirred at 0 °C for 2 h and at room temperature for 24 h. Then, distilled water (5 ml) was added into the mixture to dissolve the precipitate. The organic layer was washed with brine (15 ml) 5 times, dried over anhydrous Na_2SO_4, and then concentrated under reduced pressure to give *t*-butyl *N*-(2-aminoethyl) carbamate (EDA-Boc), appearing as thick oil (82% yield). ^{1}H NMR (400 MHz, $CDCl_3$) δ_H: 1.40 [s, 9H, C<u>H</u>$_3$ Boc], 2.80 [m, 2H, C<u>H</u>$_2$–NH$_2$], 3.20[m, 2H, CH$_2$–C<u>H</u>$_2$–NH-Boc]. FTIR (KBr disc) υ_{max}: 3360 cm^{-1} (NH stretching), 2955–2923 cm^{-1} (C–H stretching), 1693 cm^{-1} (C=O of amide stretching), 1525 cm^{-1} (NH bending), 1366-1277 cm^{-1} (C–N bending), 1172 cm^{-1} (C–O stretching).

2.2.6.2. Coupling folic acid with the amino-protected EDA. To a stirred solution of FA (0.275 g, 6.25 10^{-4} mol) in anhydrous DMSO (5 ml) and pyridine (4 ml), the solution of EDA-Boc (0.10 g, 6.25 10^{-4} mol) and DCC (0.21 g, 7.5 10^{-4} mol) in anhydrous DMSO (5 ml) were added. The mixture was stirred at room temperature for 18 h under nitrogen blanket. After the reaction completed, the mixture was gradually poured into a vigorously stirred diethyl ether (20 ml) at 0 °C. The yellow precipitate was collected and washed with cold diethyl ether several times and dried under high vacuum to obtain {*t*-butyl N-(2-aminoethyl) carbamate} folic acid (Boc-EDA-FA), appearing as a yellow solid (85% yield). ^{1}H NMR (400 MHz, DMSO-d_6) δ_H: 1.40 [s, 9H, C$\underline{H}_3$ Boc], 2.0 [m, 2H, C$\underline{H}_2$–CH$_2$–CO–NH], 2.40 [m, 2H, C$\underline{H}_2$–CO–NH], 2.90 [m, 2H, C$\underline{H}_2$–NH–CO], 3.10 [m, 2H, C$\underline{H}_2$–NH–Boc], 4.30 [m, 1H, HOOC–C$\underline{H}$–NH], 4.50 [d, 2H, phenyl-NH-C$\underline{H}_2$ folic acid], 6.60 [d, J = 8 Hz, 2H, 2CH=C$\underline{H}$ phenyl folic acid], 6.90 [t, 1H, phenyl-N$\underline{H}$-CH$_2$], 7.60 [d, J = 8 Hz, 2H, 2C$\underline{H}$=CH phenyl folic acid], 8.60 [s, 1$\underline{H}$, N=C$\underline{H}$ Ar folic acid]. FTIR (KBr disc) υ_{max}: 3360–2600 cm^{-1} (OH and $\underline{N}$H stretching), 1700 cm^{-1} (C=O of amide stretching), 1605 cm^{-1} (C–O of acid stretching), 1168 cm^{-1} (C–O stretching).

TFA (2 ml) was then added to Boc-EDA-FA and stirred at room temperature. After 2 h stirring, TFA was removed under reduced pressure and the resulting residue was dissolved in anhydrous DMF. Pyridine was added until a formation of yellow precipitate and it was subsequently washed with diethyl ether and dried to give *N*-(2-aminoethyl) folic acid (EDA-FA) (80% yield, T_m 290 °C). ^{1}H NMR (400 MHz, DMSO-d_6) δ_H: 2.0 [m, 2H, C$\underline{H}_2$–CH$_2$–CO–NH], 2.40 [m, 2H, C$\underline{H}_2$–CO–NH], 2.60 [m, 2H, C$\underline{H}_2$–NH–CO], 3.30 [m, 2H, C$\underline{H}_2$–N$\underline{H}_2$], 4.20 [m, 1H, HOOC-C$\underline{H}$-NH], 4.40 [d, 2H, phenyl-NH-C$\underline{H}_2$ folic acid], 6.60 [d, J = 8 Hz, 2H, 2CH=C$\underline{H}$ phenyl folic acid], 6.90 [t, 1H, Phenyl-N$\underline{H}$-CH$_2$], 7.70 [d, J = 8 Hz, 2H, 2C$\underline{H}$=CH phenyl folic acid], 8.60 [s, 1H, N=C$\underline{H}$ Ar folic acid]. FTIR (KBr disc) υ_{max}: 3600–2800 cm^{-1} (OH and $\underline{N}$H stretching), 1684 cm^{-1} (C=O of amide stretching), 1605 cm^{-1} (C–O of acid stretching), 1532–1335 cm^{-1} (C–N bending), 1202–1132 cm^{-1} (C–O stretching).

2.2.7. Immobilization of folic acid on the surfaces of poly(AA)-coated MNPs

Poly(AA)-coated MNPs were dispersed in a 10 ml aqueous solution containing NHS (40 mg) and EDC·HCl (20 mg) and the mixture was kept in a dark place for 2 h. The particles were recovered, washed with water and dried *in vacuo*. Then, the particles were added in a solution of 200 mg of EDA-FA and 50 mg of EDC in 10 ml anhydrous DMSO. The suspension was agitated overnight at 37 °C in dark. The particles were then recovered, washed with DMSO and methanol several times and dried *in vacuo*.

2.3. Characterization

FTIR was performed on a Perkin–Elmer Model 1600 Series FTIR Spectrophotometer. The solid samples were mixed with KBr to form pellets. Nuclear magnetic resonance spectroscopy (NMR) was performed on a 400 MHz Bruker NMR spectrometer using $CDCl_3$ as a solvent. Gel permeation chromatography (GPC) data was conducted on PLgel 10 μm mixed B2 columns and a refractive index detector. Tetrahydrofuran (THF) was used as a solvent with a flow rate of 1 ml/min at 30 °C. TEM were performed using a Philips Tecnai 12 operated at 120 kV equipped with Gatan model 782 CCD camera. TGA was performed on SDTA 851 Mettler-Toledo at the temperature ranging between 25 and 600 °C at a heating rate of 20 °C/min under oxygen atmosphere. VSM was performed at room temperature using a Standard 7403 Series, Lakeshore vibrating sample magnetometer. The magnetic moment was investigated over a range of applied magnetic fields from −10,000 to +10,000 G using 30 min sweep time. Hydrodynamic diameter of the particles was measured *via* PCS using NanoZS4700 nanoseries Malvern

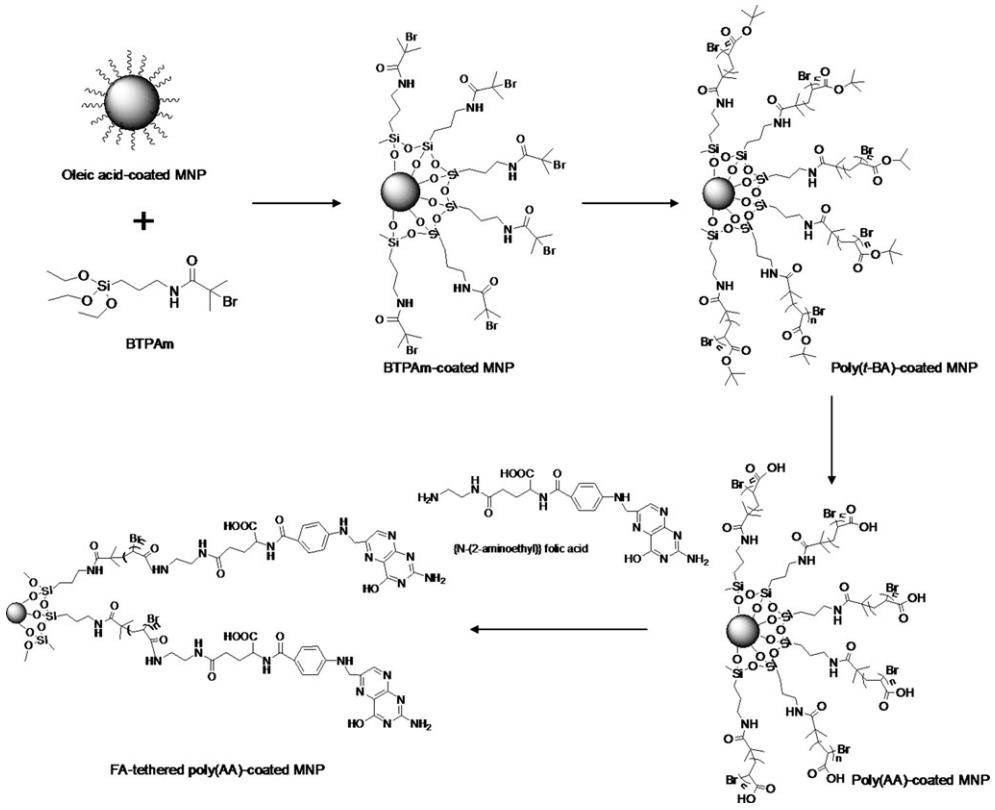

Fig. 1. Synthesis of poly(AA)-coated MNPs *via* ATRP reaction and immobilization of folic acid.

instrument. The sample dispersions were sonicated for 10 min before the measurement at 25 °C. The presence of FA was investigated using SPECORD S100 UV–Visible spectrophotometer (Analytikjena AG) coupled with a photo diode array detector at $\lambda_{max} = 371$ nm.

3. Results and discussion

The aim of this work is to modify MNP surfaces with poly(AA) and immobilize folic acid on their surfaces. Poly(AA) grafted on the particle surfaces is thought to provide steric and electrostatic stabilizations and dispersibility of the particles in aqueous media. Another major advantage of this system was that the carboxylic acid-enriched surfaces of poly(AA)-grafted MNPs provided a platform for efficient surface immobilization of any functional molecules such as DNA, drugs, protein and fluorescent molecules. Hence, the novelty of this current work is that this is the first report on synthesizing multifunctional poly(AA)-coated MNPs for attaching folic acid (FA), a model molecule in this work. Precedents have reported the immobilization of biomolecules on the distal ends of MNPs coated with other polymeric surfactant [41–44]. This novel system is hypothesized to increase the loading efficiency of FA on the MNP surfaces.

To perform surface-initiated ATRP from MNPs, BTPAm, a molecule containing an ATRP initiating site was first synthesized through amidization between APS and BIBB, followed by silanization of triethoxysilane of BTPAm on MNP surface. The results of the synthesis of BTPAm including FTIR and ^{1}H NMR are illustrated in supplementary data. To immobilize BTPAm on MNP surfaces, bare MNPs were first coated with oleic acid to form well dispersed MNPs in toluene. The advantage of this procedure was that the MNPs were well dispersible in the media before reacting with BTPAm, allowing BTPAm to effectively silanize to their surfaces due to its greater surface approaching ability in the dispersed MNPs.

Fig. 3 displays FTIR spectra of poly(*t*-BA)-coated MNPs withdrawn from the dispersions at 1, 6, 12 and 24 h of ATRP reaction. Because ATRP is known as a controlled radical polymerization, the time period for the ATRP reaction is thus crucial for tuning the molecular weight of the polymers. A progressive growth of ester linkage signals (–O(C=O)- stretching, ~1724 cm^{-1} and C–O stretching, ~1147 cm^{-1}) of *t*-BA repeating units in relative to those of a Si–O signal of the linker (~1100–1020 cm^{-1} and ~800 cm^{-1}) indicated that the molecular weights of poly(*t*-BA) on MNP surfaces increased as increasing ATRP reaction time. It should be noted that the signal corresponding to Fe-O bonds from MNP core (~589 cm^{-1}) were observed throughout the reactions without significant change in its intensity.

Weight loss from TGA technique of poly(*t*-BA)-coated MNPs at various ATRP reaction times was investigated to determine the relative amount of poly(*t*-BA) that can be grafted on the particle surface. It should be noted that the particles were separated from the uncoordinated species using an external magnet. Using an assumption that % char yield was the weight of magnetite remaining at 600 °C, the weight loss of the surface-modified MNPs was thus attributed to the decomposition of organic components including BTPAm and poly(*t*-BA) that complexed to the particle surface. Hence, percent char yield of bare MNP and MNP coated with BTPAm were determined to obtain percent of BTPAm in the complexes in each sample. According to TGA results, percent of BTPAm in the complexes was about 2 wt%, while percents of poly(*t*-BA) were 3 wt%, 15 wt%, 26 wt% and 43 wt% of the complexes at 1, 6, 12 and 24 h ATRP reaction times, respectively (Fig. 4). This was a supportive result to FTIR that poly(*t*-BA) chain length was prolonged when ATRP reaction time was extended.

To investigate the molecular weight and the molecular weight distribution of poly(*t*-BA), small amount of ethyl bromoisobutylate (EBiB) was added in the dispersion as a "sacrificial initiator" to form free poly(*t*-BA) along with poly(*t*-BA) grafted on MNP. After 24 h of

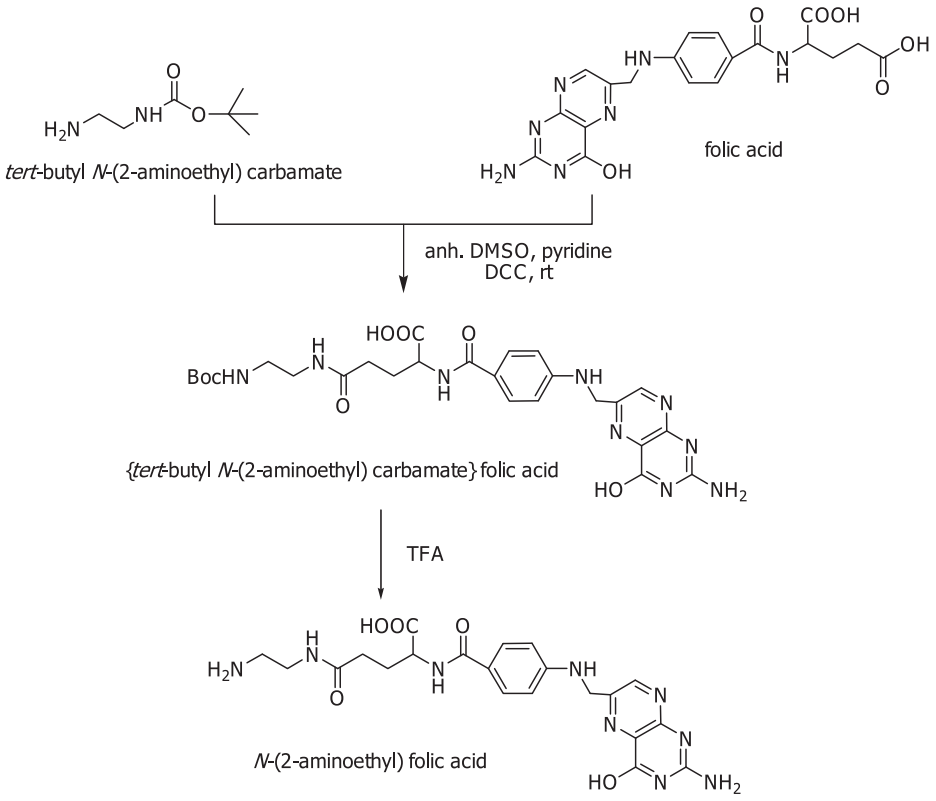

Fig. 2. Synthesis of *N*-(2-aminoethyl) folic acid (EDA-FA).

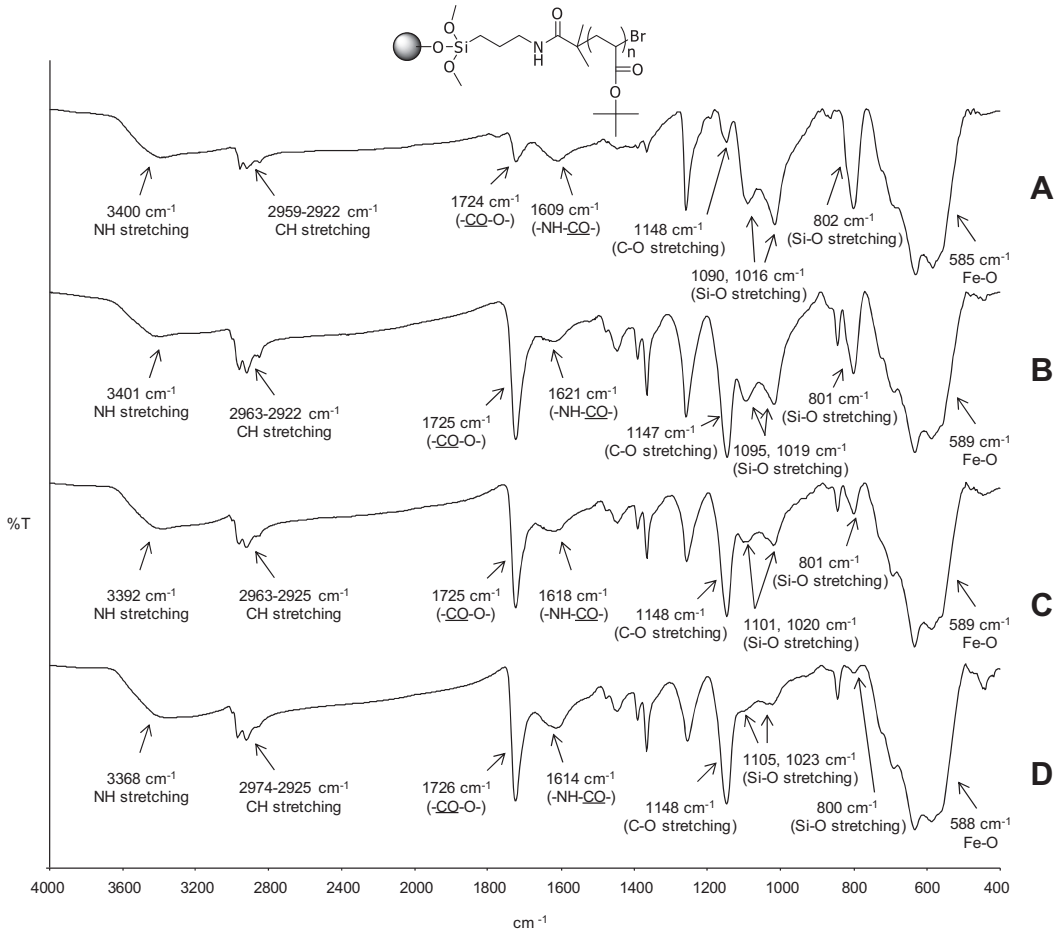

Fig. 3. FTIR spectra of poly(*t*-BA)-coated MNP at various ATRP reaction times, A) 1 h, B) 6 h, C) 12 h and D) 24 h.

the reaction, the free poly(*t*-BA) was removed from the MNP complex using an external magnet. According to GPC results, molecular weight of poly(*t*-BA) was about 18,600 g/mol and its molecular weight distribution was about 1.22. This narrow molecular weight distribution indicated the living mechanism of controlled radical polymerization. ^{1}H NMR spectrum of free poly(*t*-BA) is shown in supplementary data.

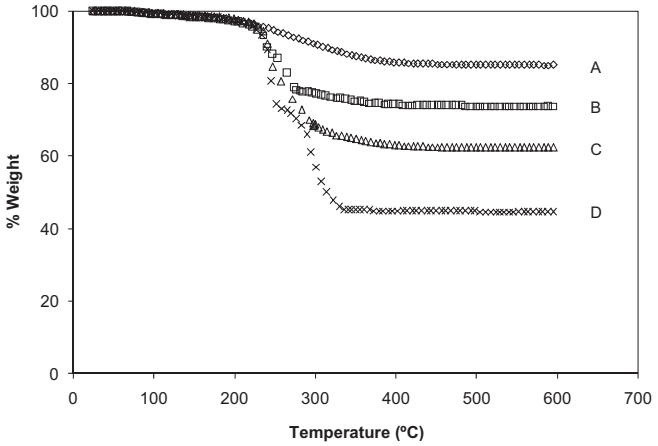

Fig. 4. TGA thermograms of poly(*t*-BA)-coated MNPs at various ATRP reaction times, A) 1 h, B) 6 h, C) 12 h and D) 24 h.

TEM images of MNP complexes at each step of the reaction are illustrated in Fig. 5. Bare MNPs observed in Fig. 5A were well organized because they were somewhat uniformed in size, which was in the range of 6–10 nm in diameter with the average of about 8 nm. Surface modification of the MNPs resulted in a slightly broader size distribution due to the presence of organic compounds coated on their surface (Fig. 5B–D). However, the average particle size was not significant difference from those of bare MNPs. It should be noted that poly(*t*-BA)-coated MNPs were well dispersed in toluene due to the existence of hydrophobic poly(*t*-BA) on their surface (Fig. 5C), while poly(AA)-coated MNPs were well dispersed in water because of the presence of hydrophilic and charge surfactants of poly(AA) (Fig. 5D).

The *M-H* curves of bare MNP, BTPAm-coated MNP, poly(*t*-BA)-coated MNPs and poly(AA)-coated MNP were illustrated in Fig. 6. They showed superparamagnetic behavior at room temperature as indicated by the absence of reminance and coercivity upon removing an external applied magnetic field. According to the results in Table 1, the decrease of saturation magnetization (M_s) from 59 emu/g of bare MNPs to 27 emu/g of poly(*t*-BA)-coated MNPs was attributed to the presence of the organic surfactant on their surface, resulting in the decrease of percent of magnetite in the complexes. After the hydrolysis of poly(*t*-BA) to form poly(AA)-coated MNP, its M_s value increased from 27 to 39 emu/g sample due to the removal of *t*-BA groups in poly(*t*-BA), which subsequently increased percent of magnetite in the complexes. Interestingly, when taking percent of magnetite in the complex into account, the M_s values in emu/g magnetite basis of these complexes were not

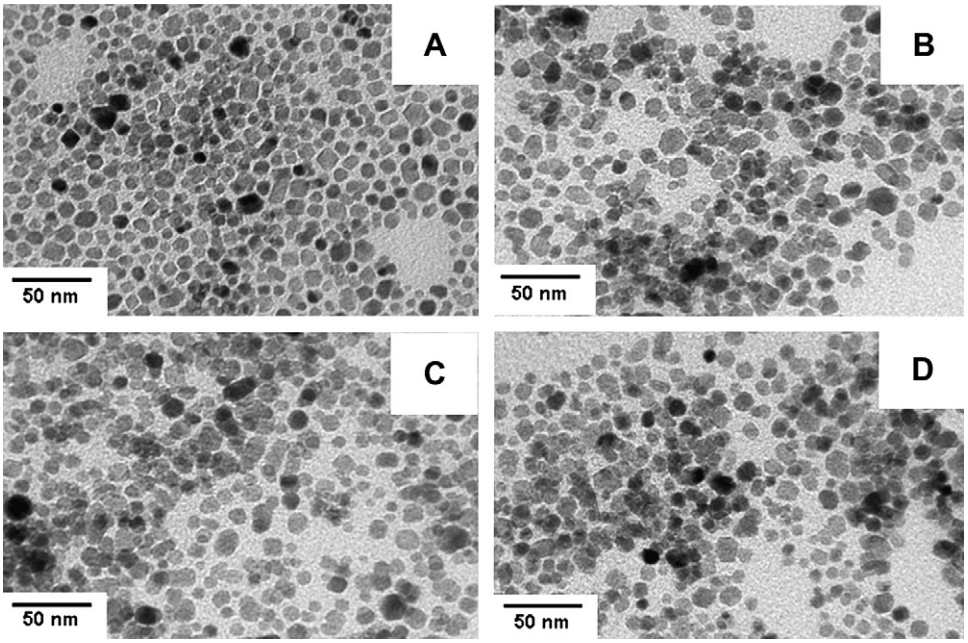

Fig. 5. TEM images of A) bare MNPs, B) BTPAm-coated MNPs, C) poly(*t*-BA)-coated MNPs, D) poly(AA)-coated MNPs. In the TEM sample preparation, MNPs in Figure A–C were dispersed in toluene and those in Figure D were dispersed in water.

significantly different from each other, indicating that magnetic properties of the particles were not considerably affected upon ATRP of poly(*t*-BA) and hydrolysis to form poly(AA)-coated MNPs.

After the hydrolysis reaction, it was conceived that MNPs having carboxylic acid-enriched surfaces were obtained. These carboxylic acid functional groups are readily reactive toward coupling reactions with other molecules having affinity functional groups such as amine and alcohol. In the current work, folic acid (FA) was chemically immobilized on the surface-modified MNPs. FA has two carboxylic acid groups at the α and γ positions, which can covalently react with amino functional groups of EDA. However, it has already been verified that γ-COOH is more accessible to covalently react with amino groups due to its high reactivity [46,47]. FA needs to be first activated with ethylene diamine (EDA) to obtain primary amine-terminated FA (*N*-(2-aminoethyl) folic acid or EDA-FA). This logical strategy enhanced the reactivity of FA to efficiently react with carboxylic acid overexpressed on the surface of poly(AA)-coated MNPs through amidization reaction. Results of the synthesis of EDA-FA including FTIR and ^{1}H NMR spectra were detailed in supplementary data.

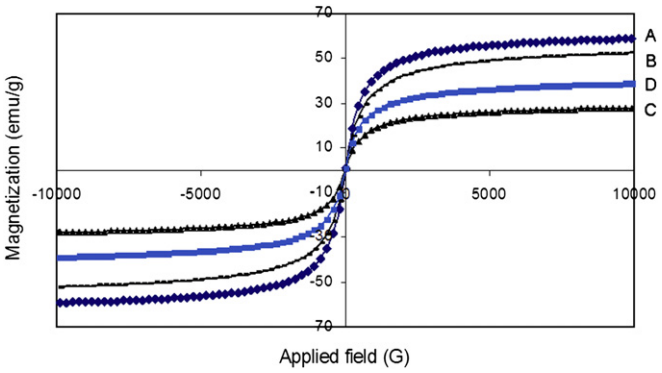

Fig. 6. *M-H* curves of A) bare MNP, B) BTPAm-coated MNP, C) poly(*t*-BA)-coated MNP and D) poly(AA)-coated MNP.

In the grafting reaction between poly(AA)-coated MNPs and EDA-FA, *N*-hydroxyl succinimide (NHS) was used to activate the dangling carboxylic acid groups. FTIR spectra of the products in each step were thus illustrated in comparison with the starting compounds (Fig. 7). Fig. 7A showed the FTIR spectrum of poly(AA)-coated MNPs and those of NHS was depicted in Fig. 7B. In Fig. 7C, the sharp and strong characteristic signal of ester linkages appeared at 1723 cm^{-1}, indicating the coupling reaction between carboxylic acid of poly(AA)-coated MNPs and NHS. In addition, Fe-O linkages of magnetite core were also observed at 586 cm^{-1}. After the coupling reaction with EDA-FA (Fig. 7D), the characteristic signals of FA, such as 1700–1500 cm^{-1} and 1153–1069 cm^{-1}, appeared in the FA-bound MNPs (Fig. 7E), indicating the successful conjugation of FA on the MNP surfaces.

UV–visible spectrophotometry was also applied to confirm the presence of FA in the conjugated MNP complex. FA showed a λ_{max} value at 371 nm (Fig. 8A), whilst those of FA-conjugated MNPs also exhibited a weak absorbance signal at the same wavelength (Fig. 8B). It is worth to mention that poly(AA)-coated MNPs before FA loading did not show any absorbance signal at the same wavelength (Fig. 8C). This result implied that FA was, to some extent, covalently conjugated to the MNP surfaces.

To determine percentage of magnetite core and organic shell in the complexes in each step of the reactions, the complexes were characterized *via* TGA to investigate their mass loss. Bare MNPs manifested a drastic weight loss between 200 and 350 °C with 90%

Table 1
Percentage of magnetite in the complex and their magnetic properties.

Sample	emu/g sample[a]	% Fe_3O_4[b]	emu/g Fe_3O_4
Bare MNP	59	90	65
BTPAm-coated MNP	53	88	60
Poly(*t*-BA)-coated MNP	27	45	61
Poly(AA)-coated MNP	39	63	62

[a] Estimated from the saturation magnetization (M_s) at 10,000 G from VSM technique.
[b] Estimated from % char yield at 600 °C from TGA technique.

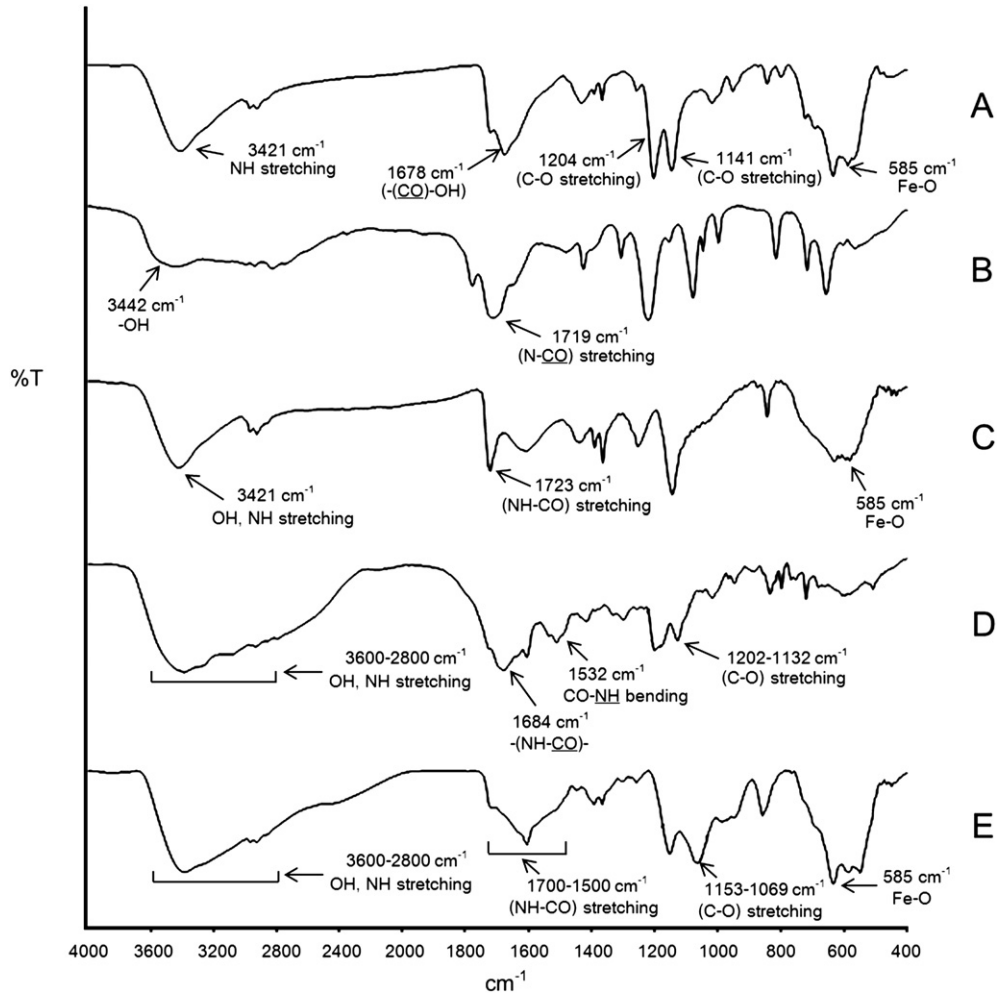

Fig. 7. FTIR spectra of (A) poly(AA)-coated MNP, (B) NHS, (C) NHS-poly(AA)-coated MNP, (D) EDA-FA and (E) FA-poly(AA)-coated MNP.

char yield (Fig. 9A). This was attributable to the decomposition or desorption of the absorbed ammonium salt at elevated temperature and eventually loss some weight [48,49]. The weight loss of MNPs coated with BTPAm, poly(*t*-BA) and poly(AA) were attributed to the decomposition of organic components complexing to the particle surface and % char yields were the weight of magnetite core. From TGA thermograms in Fig. 9B,C, there was about 2 wt% of BTPAm and 49 wt% of poly(*t*-BA) in poly(*t*-BA)-coated MNPs. The

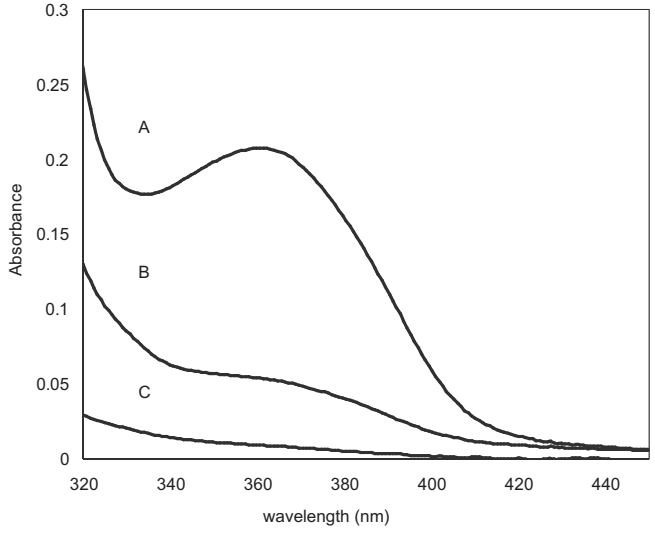

Fig. 8. UV–visible spectra of (A) folic acid (FA), (B) FA-conjugated MNP and (C) poly (AA)-coated MNP without FA.

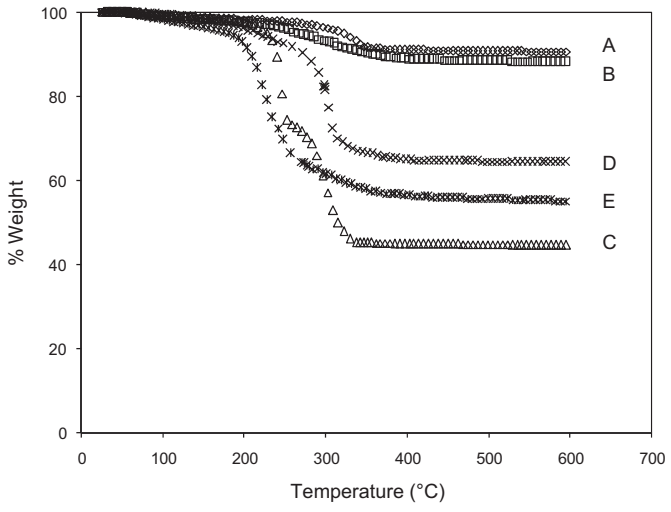

Fig. 9. TGA thermograms of (A) bare MNP, (B) BTPAm-coated MNP, (C) poly(*t*-BA) coated MNP, (D) poly(AA)-coated MNP and (E) FA-poly(AA)-coated MNP.

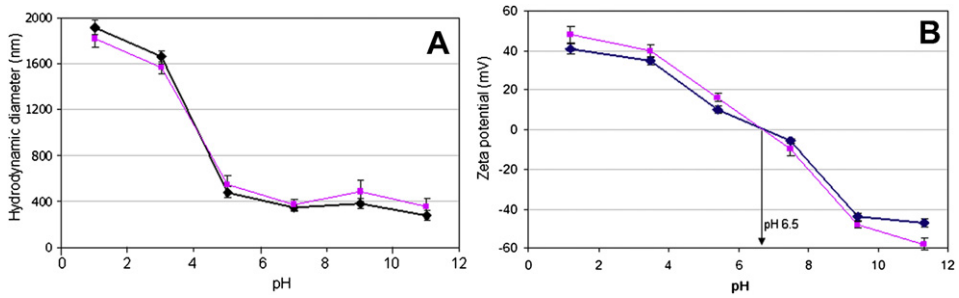

Fig. 10. The effect of pH of the aqueous dispersions containing poly(AA)-coated MNP (◆) and FA-poly(AA)-coated MNP (■) on their hydrodynamic diameter and zeta potential. The experiments were performed at 25 °C.

grafting density of BTPAm, the initiating site for ATRP on the particle, can be calculated and it was found that there was about 0.8 molecule/nm^2 (150 molecules/particle). Examples of the calculation are illustrated in supplementary data. The grafting density of poly(*t*-BA) were comparable to that of BTPAm on the surface.

After the hydrolysis of poly(*t*-BA), percent of organic components in the case of poly(AA)-coated MNPs significantly dropped (from 49 to 27 wt%) due to the removal of *t*-BA groups from the polymeric layer of the particles (Fig. 9D). The 27 wt% of poly(AA) corresponded to 23 carboxylic acid/nm^2 (4600 acid/particle). From Fig. 9E, there was about 14 wt% of FA in the complex, corresponding to about 2 FA molecules/nm^2 (400 FA molecules/particle). Therefore, percent conversion of carboxylic acid to FA was about 8%. The lowering temperature of TGA curve in Fig. 9E (FA-poly (AA)-coated MNP) as compared to that in Fig. 9D (poly (AA)-coated MNP) was attributed to the weight loss of FA component in the complex. The decomposed TGA thermogram of free FA has been investigated and shown in supplementary data. In addition, it was also found that there was about 2.7 FA molecules/site of the ATRP initiator (400 FA molecule/150 sites of BTPAm in a single particle). The limited number of the % conversion and grafting density of FA on the particle surface was attributed to limited accessibility of bulky FA to react with steric poly (AA). However, the grafting density of FA might be improved by copolymerization of poly(AA) with other polymers to lessen steric hindrance of the compact poly(AA), so that FA con be more effectively conjugated. Also, utilization of spacer from the particle surface is another approach that can diminish steric hindrance on the dense surface.

Because carboxylic acid functional groups can be easily ionized in an aqueous solution, it is thus interesting to understand how pH of the dispersions affect hydrodynamic diameter and surface charge of poly(AA)-coated MNPs and FA-poly(AA)-coated MNP. pH of the aqueous dispersions containing the complexes (0.2 mg/ml) were varied from approximately 1–11 and their hydrodynamic diameters were determined *via* PCS technique. In both samples, as pH of the dispersions increased, their hydrodynamic diameters rapidly decreased at acidic pH (ranging between pH 1.2–5.4) and gradually decreased at pH ranging between 5.4 and 11.3 (Fig. 10). It was hypothesized that as increasing pH of the dispersions, ionization of carboxylic acid on the surface of poly(AA)-coated MNPs took place, resulting in the formation of carboxylate ions on their surfaces. The negative charges of carboxylate ions led to additional electrostatic repulsion toward neighboring particles and thus prevented massive flocculation.

The results from zeta potential measurements also supported this assumption. The surface charges of poly(AA)-coated MNPs were positive at the pH ranging between 1.2 and 6.5 and negative at the pH range of 6.5–11.3, implying that point of zero charge (PZC) of this complex was pH 6.5 (Fig. 10). It was also found that FA-containing complex showed a slightly higher zeta potential than the other at pH ranging between 1.2 and 6.5. This was attributed to the presence of amines in FA structure, resulting in protonated amino groups. Similarly, the enriched amines in the complex might also influence the lower zeta potential in FA-containing complex at basic pH.

The large size of the particles in DLS as compared to those from TEM measurements (8 nm in diameter) might come from the fact that there were some nano-clusters of particles in the dispersions. These nano-clusters of the particles can be observed in TEM measurements from the first step of the particle synthesis (shown in supplementary data). When poly(AA) was chemically grafted on their surface, these clusters still presented. Although these nano-clusters existed in the dispersions, the particles were well dispersible in aqueous dispersions without macroscopic aggregation visibly observed because there were poly(AA) coated on their surface.

Cytotoxicity testings of poly(AA)-coated MNP and FA-poly(AA)-coated MNP were also performed. According to our preliminary results, it was found that the dispersions were not toxic against Vero cell line up to 50 μg/ml concentration of the sample (sulforhodamine B (SRB) assay method). Detail studies regarding the toxicity of the magnetite complexes are warranted for future studies.

4. Conclusions

This work presented a “grafting from” strategy to modify MNP surfaces with poly(*t*-BA) *via* ATRP, followed by a hydrolysis of *t*-BA groups to obtain poly(AA) and finally immobilization of folic acid on their surfaces. The originality of this work is that this is the first report on modifying MNP surface with poly(AA) which serves as a platform for folic acid immobilization. Because the folate receptor is overexpressed on the surface of cancer cells, it is for this reason that folic acid is of particular interest in the current work in an attempt to facilitate the intracellular uptake by specific cancer cells for cancer therapy. Folic acid was successfully activated with ethylene diamine (EDA) to obtain primary amine-terminated folic acid derivative. This logical strategy enhanced the reactivity of folic acid to be efficiently immobilized on MNP surfaces through amidization reaction.

In addition to the use of binding affinity of carboxylic acid functional groups, poly(AA) on their surface can also provide stabilization mechanisms through both steric repulsion due to the long chain polymers and electrostatic repulsion owing to the formation of negative charges in basic pH dispersions. Furthermore, poly(AA) on their surfaces also promoted particle dispersibility in water, which is a minimum requirement for biomedical uses. This novel magnetically guidable nanocomplex might be suitable for use as an efficient drug delivery vehicle particularly for cancer treatment.

Acknowledgement

The authors thank the Thailand Research Fund (TRF) and Naresuan University (DBG5380001) for financial funding. The Center of Excellence for Innovation in Chemistry (PERCH-CIC), Commission on Higher Education, Ministry of Education is also gratefully acknowledged for financial support.

Appendix. Supplementary data

Proposed reaction mechanisms of trifluoroacetic acid (TFA) with the polymers on MNP surface. FTIR and ^{1}H NMR spectra of 2-bromo-2-methyl-*N*-(3-(triethoxysilyl) propanamide (BTPAm)) and *N*-(2-aminoethyl) folic acid (EDA-FA). ^{1}H NMR spectrum of poly(t-BA), TEM images showing some nano-aggregation. Examples of calculation of grafting density. TGA thermogram of folic acid.

Appendix. Supplementary data

Supplementary data associated with this article can be found in the online version, at doi:10.1016/j.polymer.2010.12.059.

References

[1] Pei W, Kumadaa H, Natusmea T, Saitoa H, Ishio S. J Magn Magn Mater 2007;310:2375–7.
[2] Sun S, Murray CB, Weller D, Folks L, Moser A. Science 2000;287:1989–92.
[3] Teng X, Yang H. J Am Chem Soc 2003;125:14559–63.
[4] Casula MF, Floris P, Innocenti C, Lascialfari A, Marinone M, Corti M, et al. Chem Mater 2010;22:1739–48.
[5] Anders S, Sun S, Murray CB, Rettner CT, Best ME, Thomson T, et al. Microelectron Eng 2002;61-62:569–75.
[6] Woo K, Hong J, Choi S, Lee HW, Ahn JP, Kim CS, et al. Chem Mater 2004;16:2814–8.
[7] Zhang J, Misra RDK. Acta Biomater 2007;3:838–50.
[8] Laurent S, Forge D, Port M, Roch A, Robic C, Elst LV, et al. Chem Rev 2008;108:2064–110.
[9] Veiseh O, Gunn JW, Zhang M. Adv Drug Deliv Rev 2010;62:284–304.
[10] Sahoo Y, Goodarzi A, Swihart MT, Ohulchanskyy TY, Kaur N, Furlani EP. J Phys Chem 2005;109:3879–85.
[11] Hayashi K, Ono K, Suzuki H, Sawada M, Moriya M, Sakamoto W, et al. Chem Mater 2010;22:3768–72.
[12] Feng PB, Gao F, Gu HC. J Colloid Interface Sci 2005;284:1–6.
[13] Liu X, Xing J, Guan Y, Shan G, Liu H. Colloids Surf A Physicochem Eng 2004;238:127–31.
[14] Mornet S, Vekris A, Bonnet J, Duguet E, Grasset F, Choy JH, et al. Mater Lett 2000;42:183–8.
[15] Cheng G, Zhao J, Tu Y, He P, Fang Y. Anal Chem Acta 2005;533:11–6.
[16] Lellouche J, Senthil G, Joseph A, Buzhansky L, Bruce I, Bauminger ER, et al. J Am Chem Soc 2005;127:11998–2006.
[17] Corr SA, Rakovich YP, Gun'ko YK. Nanoscale Res Lett 2008;3:87–104.
[18] Zhang Y, Kohler N, Zhang M. Biomaterials 2002;23:1553–61.
[19] Sonvico F, Mornet S, Vasseur S, Dubernet C, Jaillard D, Degrouard J, et al. Bioconjug Chem 2005;16:1181–8.
[20] Zhoua Y, Wang S, Ding B, Yang Z. Chem Eng J 2008;138:578–85.
[21] Fischer H. Chem Rev 2001;101:3581–610.
[22] Pyun J, Jia S, Kowalewski T, Patterson GD, Matyjaszewski K. Macromolecules 2003;36:5094–104.
[23] Hu B, Fuchs A, Huseyin S, Gordaninejad F, Evrensel C. Polymer 2006;47:7653–63.
[24] Zhao H, Shipp DA. Chem Mater 2003;15:2693–5.
[25] Liu G, Yan X, Lu Z, Curda SA, Lal J. Chem Mater 2005;17:4985–91.
[26] Sun Y, Ding X, Zheng Z, Cheng X, Hu X, Peng Y. Euro Polym J 2007;43:762–72.
[27] Hermann High LR, Holder SJ, Penfold HV. Macromolecules 2007;40:7157–65.
[28] Shipp DA, Wang JL, Matyjaszewski K. Macromolecules 1998;31:8005–8.
[29] Xia J, Gaynor SG, Matyjaszewski K. Macromolecules 1998;31:5958–9.
[30] Teodorescu M, Matyjaszewski K. Macromolecules 1999;32:4826–31.
[31] Raghuraman GK, Rühe J, Dhamodharan R. Nanopart Res 2008;10:415–27.
[32] Czaun M, Hevesi L, Takafuji M, Ihara H. Chem Commun; 2008:2124–6.
[33] Marutanil E, Yamamoto S, Ninjbadgar T, Tsujii Y, Fukuda T, Takano M. Polymer 2004;45:2231–5.
[34] Zhou Y, Wang S, Ding B, Yang Z. Chem Eng J 2007;40:6217–23.
[35] Fan QL, Neoh KG, Kang ET, Shuter B, Wang SC. Biomaterials 2007;28:5426–36.
[36] Frimpong RA, Hilt JZ. Nanotechnology 2008;19:1–7.
[37] Si S, Kotal A, Mandal TK, Giri S, Nakamura H, Kohara T. Chem Mater 2004;16:3489–96.
[38] Zhang M, Breiner T, Mori H, Muller AHE. Polymer 2003;44:1449–58.
[39] Wan S, Zheng Y, Liu Y, Yan H, Liu KJ. Mater Chem 2005;15:3424–30.
[40] Sauzedde F, Elaïssari A, Pichot C. Colloid Polym Sci 1999;277:846–55.
[41] Ng V, Lee YV, Chen BT, Adeyeye AO. Nanotechnology 2002;13:554–8.
[42] Hayashi K, Moriya M, Sakamoto W, Yogo T. Chem Mater 2009;21:1318–25.
[43] Kohler N, Fryxell GE, Zhang M. J Am Chem Soc 2004;126:7206–11.
[44] Landmark KJ, DiMaggio S, Ward J, Kelly C, Vogt S, Hong S, et al. ACS Nano 2008;2:773–83.
[45] Pinna N, Grancharov S, Beato P, Bonville P, Antonietti M, Niederberger M. Chem Mater 2005;17:3044–9.
[46] Mohapatra S, Mallick SK, Maiti TK, Ghosh SK, Pramanik P. Nanotechnology 2007;18:385102.
[47] Park EK, Lee SB, Lee YM. Biomaterials 2005;26:1053–61.
[48] Rutnakornpituk M, Meerod S, Boontha B, Wichai U. Polymer 2009;50:3508–15.
[49] Tao K, Dou H, Sun K. Chem Mater 2006;18:5273–8.